Chapter 4
Observational Links Between Fermi-LAT Pulsars and Their Nebulae

Emma de Oña Wilhelmi

Abstract GeV pulsar and TeV pulsar wind nebulae represent the largest Galactic population in the GeV and TeV regime respectively. Even when sharing the same central engine, that is, an energetic and young pulsar, the processes ruling the two regimes differ greatly. At GeV energies, the radiation is pulsed and the environment conditions on the pulsar magnetosphere and pulsar wind prevail. At TeV energies, the steady, integrated over time, nebula outshines. Nevertheless those processes should be ultimately connected being different aspects from a continuous pulsar/PWNe system. We review the state-of-the-art knowledge on these objects and describe in a quantitative manner the general trends observed experimentally, which will be further investigated.

4.1 Introduction

Pulsars or rotating neutron star are highly magnetised, fasting-rotating (ms to s) compact objects which emit radiation in all wavelength, even up to several tens of TeVs, offering an opportunity to study physic processes under extreme conditions. Along with electromagnetic emission, pulsars dissipate their rotational energy via relativistic winds of particles. Since the relativistic bulk velocity of the wind is supersonic with respect the ambient medium, such a wind produce a termination shock. The wind particles, moving through the magnetic field and the ambient photons, produce radiation that we observe as pulsar wind nebulae (PWNe). As the pulsars themselves, the PWN emits at all wavelengths from radio to TeV. The complex involving pulsars, their winds and, eventually, a surrounding supernova blast (see Fig. 4.1) covers a wide range on dimension scales, from a few kilometres to more than 20 pc in some cases. The small region comprised by the light cylinder (with typical size of $\sim 10^9$ cm) that surrounds the rotating $\sim 10^6$ cm-radius star, confines an exceptionally energetic magnetised plasma, with magnetic field strengths as high as $B \sim 10^{9-12}$ G. This small volume, however, drives the particle

E. de Oña Wilhelmi (✉)
Institute of Space Sciences, (IEEC-CSIC) Campus UAB, Carrer de Can Magrans, s/n, Catalonia, Spain
e-mail: wilhelmi@ice.csic.es

D.F. Torres (ed.), *Modelling Pulsar Wind Nebulae*, Astrophysics and Space Science Library 446, DOI 10.1007/978-3-319-63031-1_4

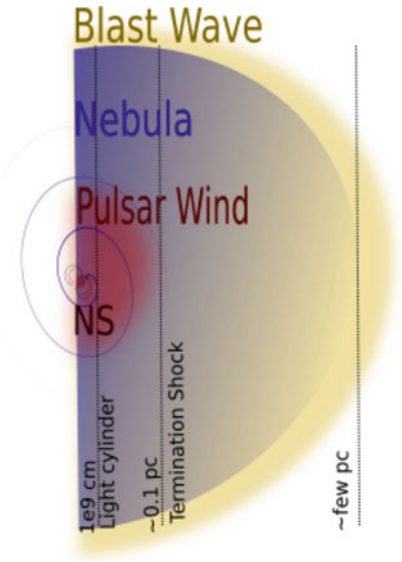

Fig. 4.1 Schematic view of a pulsar, its pulsar wind nebulae and hosting supernova remnant

flow that surrounds it, forming a relativist winds that extends up to ∼0.1 pc. At even larger scales, reaching tens of parsecs in evolved systems or PWN embedded in regions of low density, the wind inflates a large bubble of particles and magnetic field, forming the magnetised nebula, which is at the same time strongly affected by the shock blast left behind by the supernova explosion. The understanding of pulsars and their nebula requires thus not only a multi-wavelength approach but also the study of transport mechanisms and cooling processes at very different length scales.

Since 2005, pulsar and PWN astrophysical research at high energies has experienced a veritable revolution, mainly driven by the increase of the sample of those sources at GeV and TeV energies, from a handful to a few tens or hundreds (in case of PWNe and pulsars respectively). The first five high energy pulsars were detected by the *Energetic Gamma-Ray Experiment Telescope* (EGRET) at energies $E > 100$ MeV. Crab, Vela, Geminga, PSR B1055−52, PSR B1706−4 and PSR B1951+32 (Nolan et al. 1996) were clearly identified through their timing signature, whereas several of the 271 EGRET unidentified sources were also believed to be related to pulsars and millisecond pulsars (see Thompson et al. 2005 for a review). Regarding their nebulae, only one source was established before 2005: the Crab nebula discovered in 1989 (Weekes et al. 1989). Interestingly, the flux measured from the Crab nebula has been used as the standard candle in very-high energy astronomy ever since, nonetheless recent observations with high sensitivity instruments have revealed a rich and complex phenomenology on its (previously believed to be) steady emission (see Zanin and Acero contributions in this book). Concerning pulsars, this scenario dramatically changed with the advent of more sensible detectors in satellites at GeV such *AGILE* (Astro-rivelatore Gamma a Immagini LEggero) (Tavani 2011) in 2007 and specially with the Fermi Gamma-ray Space Telescope (*Fermi*) (Atwood et al. 2009) with the LAT (Large Area

Telescope) instrument on board, launched in 2008. The number of pulsars detected by summer 2016 amounts 161 (Johnson et al. 2014), allowing the study of both individual and collective properties of the pulsar population. Several competing gamma-ray pulsars models (see next section for a short review based on Takata et al. (2006); Muslimov and Harding (2004); Romani and Yadigaroglu (1995); Grenier and Harding (2015); Kalapotharakos et al. (2016) and references therein) have been contrasted with the high-energy pulsar population, predicting their spectral features and light curves according to their birth properties, beaming and evolution (Gonthier et al. 2007; Watters and Romani 2011; Pierbattista et al. 2016). Those comparisons favor models in which the gamma-ray emission is originated in the outer part of the magnetosphere and they also require a large amount of pairs (electrons and positron) to sustain the radiation level. Even when they can reproduce many of the average radio and high-energy characteristics, they also highlight significant differences, as for instance the need to call of different regions/mechanisms to explain different light-curve structures. Alongside to those discoveries and theoretical development in the GeV regime, a number of high-sensitive, good-imaging Cherenkov telescope arrays have been exploring the TeV sky, resulting on a dramatically increase of the number of TeV-emitting sources on the Galactic plane. Observations with MAGIC, Veritas and H.E.S.S. telescope arrays and their upgrades have revealed 72 new TeV sources lying on the Galactic plane.[1] Out of them, 35 are classified as PWNe, although only 19 are firmly identified (based mainly on their multi-wavelength properties). In particular, the Galactic plane survey performed by the H.E.S.S. collaboration from 2005 until 2015 has allowed a complete population study on nebulae associated with bright pulsars, in a region defined by a range of longitude between 250° and 65° and narrow latitude strip of −3.5° and 3.5°.

Fed by the large amount of information provided by satellites and ground-based telescopes, theoretical and phenomenological models have dramatically evolved. However, the interplay and relations connecting the pulsed emission, which dominates in the MeV and GeV regime and the non-pulsed emission of the nebula, which dominates at TeV energies, are still far from being solved. The first seems to be regulated by the freshly injected electron and positron wind in the pulsar magnetosphere, and its propagation towards the termination shock. In the second, the gamma-ray emission detected relates to the integrated wind along the pulsar lifetime and it is subject to changes in the environment around the pulsar (i.e. the evolution within the hosting SNR or the region in which the explosion occurred). Several excellent summaries on the status of GeV pulsar observations can be found in i.e. Ray and Parkinson (2011); Caraveo (2014); Grenier and Harding (2015); Breed et al. (2016). Likewise, a throughout review on PWN was provided by several authors (i.e. Kargaltsev et al. 2013; de Oña Wilhelmi 2011; Gallant et al. 2008). Here, we intend to emphasise the link between the two populations, focusing in the shared energetic and environmental aspects that connect the different spectral features they display.

[1] http://tevcat2.uchicago.edu/.

In Sect. 4.2 we will outline the state-of-the-art of pulsar modelling and latest simulations. Likewise, we will summarise the current knowledge of PWNe, emphasising the main problems we face on the PWNe field. In Sect. 4.3 we will discuss the general properties of pulsars and PWNe populations and their interplay. In Sect. 4.4 we report on new types of pulsars and PWNe and how do they tally with the known populations. Finally the last Section will be devoted to the usual general discussion.

4.2 High-Energy Pulsars and Their Relativistic Winds

The standard pulsar paradigm to explain pulsed emission from neutron stars relies in acceleration of particles in low-density plasma regions or gaps within the pulsar magnetosphere. Those particles loose energy via synchrotron-curvature processes when they travel along the strong magnetic field lines. Different altitudes and regions in the magnetosphere were proposed to explain the origin of the multi-wavelength pulsed emission observed: at low altitude above the star, usually attribute to radio pulses, or further out near the light cylinder. This cylinder is defined by the radius $R_{\rm LC} = c/\Omega$ from the spin axis, beyond which the field lines cannot co-rotate with the neutron star without violating the speed of light, but instead they spiral outwards forming a cold, relativistic wind (see Fig. 4.2). The resolution of

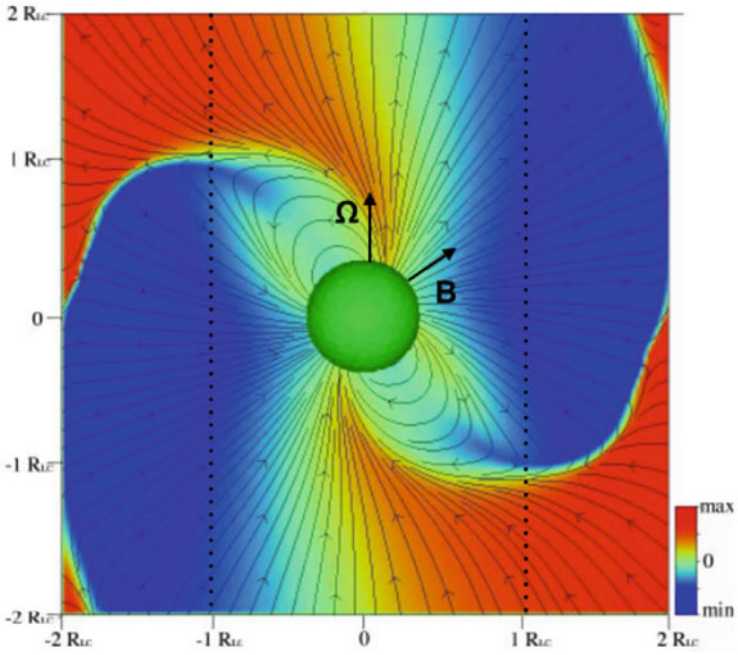

Fig. 4.2 *Magnetic field lines* obtained from MHD simulations of an oblique pulsar magnetosphere with magnetic inclination of 60° in the corotating frame plane (Spitkovsky 2006). *Color* represents the magnetic field perpendicular to the plane

force-free magnetosphere plasma models (Tchekhovskoy et al. 2016; Contopoulos 2016; Cerutti et al. 2016) can trace how currents are located in the surrounding of pulsars. Earlier models treated the magnetosphere as a vacuum, locating the acceleration and high-energy emission either above the pulsar caps (polar cap models), near the light cylinder (outer gap models) or along the last open field lines from the neutron star surface to near the light cylinder (slot gap). They appeal to synchrotron-curvature (SR, CR) mechanisms from primary and secondary electrons and positrons, as well as self-synchrotron Compton (SSC) in some particular cases, to explain the broad-band emission of pulsars.

The field is quickly evolving, thanks in part to the better computational power but mainly driven by the large date set of experimental results supplied in last years. New particle-in-cell (PIC) and magneto-hydro-dynamic (MHD) simulations are being currently developed, showing a quite different picture. This two approaches are based on either solving self-consistently electromagnetic fields, current and charge densities of a rotating star with a dipole moment through MHD simulations, or computing the individual particle response to the electromagnetic fields, through N-body simulations, or through PIC simulations that also compute the self-consistent change in the fields due to the particles. In recent MHD simulations of dissipative pulsar magnetospheres (Cerutti et al. 2016) (that is, including a parallel electric field, away from ideal MHD simulations), the interplay between the magnetosphere and the relativist pulsar wind, which blows away from the pulsar, plays an important role. By solving the electromagnetic structure of an oblique magnetosphere, including particle acceleration, and the emission of radiation self-consistently, in a 3D spherical particle-in-cell simulations, current sheets appear either along the last closed magnetosphere magnetic lines, and/or on the equatorial plane, extending beyond the magnetosphere. These current sheets are optimal places for magnetic reconnection to happen (Cerutti et al. 2016; Mochol and Pétri 2015) and have been suggested as origin of the gamma-ray emission at GeV and TeV, even beyond the magnetosphere. According to those models, young pulsars with high magnetic field and strong pair production are weakly dissipative whereas in old ones, the current sheets are dominated by the equatorial ones on the wind zone. When the rotator is oblique, naturally these sheets corrugate producing a striped wind in which particles can also undergo relativistic magnetic reconnection and emit gamma-rays via self-synchrotron-Compton (Pétri 2015; Mochol and Pétri 2015). Those stripped winds are also believed to depend on the pulsar age, becoming radiative-dominant (young ones, such as the Crab pulsar), or escaping-dominant (older pulsars such as Vela pulsar). A different mechanism for pulsed emission at high and very-high energies was proposed by Aharonian et al. (2012), in which the relativistic winds becomes kinetic dominant, transferring energy for the strong magnetic field to particles, and off-scattering pulsed optical and X-ray photon fields. As a results, a new Compton component will mimic the low energy timing signature (if close enough to the light cylinder) emerging above a few tens of GeV. Although these models in general satisfactorily explain light curves and phase-resolved spectra at GeV energies, they also suffer from some drawbacks, such the maximum Lorenz factor achieved, the lack of unscreened electric field in an ideal MHD or the origin of the supply charges.

4.3 Beyond the Wind: The Pulsar Wind Nebulae

PWNe are bubbles of relativistic particles and magnetic field formed by the interaction of the relativistic pulsar wind with the surrounding Supernova Remnant (SNR) or the interstellar medium (ISM). Models connecting the pulsed emission with the pulsar wind correlate with the structure of the surrounding nebula for young pulsars. Instead, in the case of evolved ones, the morphology and energetics of the PWN is strongly modified by first the interaction with the hosting SNR and then by the expanding within the surrounding medium of the nebula along the years. Upon passing through the termination shock, the wind kinetic energy is randomised, and the purely toroidal magnetic field is carried out and accumulates within the volume of the nebula. Since Kennel and Coroniti (1984) published the first MHD description of the plasma flow in the Crab Nebula, there has always been an unexplained ingredient in the pulsar to nebula modelling: the low level of magnetisation of the flow immediately upstream of the pulsar wind termination shock. This is what is commonly referred to as the σ-problem: the pulsar wind, carrying most of the rotational energy lost by the pulsar, is Poynting-dominated (highly magnetised) at its base, while MHD modelling of PWNe requires it to be particle dominated at the shock. 2D MHD simulations (Komissarov and Lyubarsky 2004; Del Zanna et al. 2006) somewhat alleviated the strong requirements of the (Kennel and Coroniti 1984) model, and more recently 3D MHD simulations (Porth et al. 2014) have suggested that actually an equal amount of energy in particles and field at the shock might be required to reproduce the Crab Nebula morphology. This latter conclusion, however, comes from the idea that, thanks to kink instabilities, the magnetic field becomes progressively more tangled and dissipates in the bulk of the nebula, i.e. in the radiation region, rather than in the cold pulsar wind. Unfortunately, observations of the pulsar wind are hampered by its own nature, being cold and ultra-relativistic. However, the recent developments on pulsar physics related to the location of the pulsed emission regions, extending beyond the magnetosphere, have opened a new line of research, in which high energy observations, and in particular observations of pulsed emission above 100 GeV, might unveil a new inverse Compton component, and therefore pinpoint a region where the wind evolved from a magnetic-dominant to a kinetic-dominant wind, transferring the energy injected by the pulsar to particles which can be accelerated and up-scatter soft photon fields.

Detailed morphological studies of PWNe with high-resolution X-ray satellites such as Chandra have revealed complex structures in these nebulae. In general, young pulsars show an axial symmetry around what is believe to be the pulsar rotation axis, interpreted as a result of the latitude dependence of the pulsar wind energy flux (Lyubarsky 2002; Komissarov and Lyubarsky 2003; Del Zanna et al. 2004; Bogovalov and Tsinganos 2005), whereas some of the more evolved systems show a crushed morphology, resulting from the interaction with the host SNR. Prominent examples such Crab and Vela can be described satisfactorily using 2D and 3D simulations, but they fail to reconstruct the multi-wavelength spectrum (Aleksić et al. 2015; Abramowski et al. 2012). On the other hand, spatially

independent models in which the time evolution of the electron spectrum is taking into account (Martín et al. 2012; Tanaka and Takahara 2013; Fang and Zhang 2010; Gelfand et al. 2009) can fit the global spectrum of PWNe, by assuming different injection electron spectral shape, contribution of photon field (namely far infra-red, near infra-red and CMB background) and magnetic field strengths. Those models can unveil general trends, but they fail to explain satisfactorily the particular details of the observed emission, in particular in X-rays and TeV energies. This is the case even for the Crab nebula, which exhibits the strongest flux, for which dedicated models applied to the latest results obtained with the MAGIC telescopes (Aleksić et al. 2015) cannot reproduced the broadband shape. In general, the assumption of a constant magnetic field dominating the inverse Compton emission is not realistic. Instead a turbulent medium in the nebula magnetic field could explain some of the features observed in TeV PWNe, including the, in some objects, extremely low magnetic field required to adjust the X-ray and TeV flux level (see i.e. H.E.S.S. Collaboration et al. 2012). A two-folded approach, in which the proper time-dependent radiative mechanisms are combined with MHD realistic simulations seems to be providing answers on the correct direction, although the complexity of the morphology in evolved PWNe and computational expensive modelling is still a challenge.

4.4 Connecting Pulsars and PWNe

Observations of gamma-ray pulsars have been strongly boosted after the launching of the AGILE satellite and, specially, the *Fermi* satellite in 2007–2008. The gamma-ray telescopes on board of these satellites are sensitive to energies above 60 MeV and have allowed the discovery of more than 160 pulsars (Abdo et al. 2013) (see Fig. 4.3). From those, 61 were known prior through radio or X-ray observations, and typified as young radio loud pulsars (YRL). Thanks to both, the good sensitivity of the instrument and the strong flux of these sources, many of the, in principle, unidentified sources were revealed to be pulsars via the discovery of periodic signals using blind searches techniques (and dubbed young radio quiet, YRQ, pulsars) (Abdo et al. 2009). The gamma-ray emission is believed to originated in beam-like regions that sweep the sky co-rotating with the neutron star. In general, these beams seem to be wider than the radio emission beams, increasing thus the probability to intersecting with the line of sight and resulting on a *loud* gamma-ray emitter but *quiet* radio pulsar. Finally, a large fraction of the pulsars reported on the catalog (39) are classified as millisecond pulsars (MSPs) (Grégoire and Knödlseder 2013), a hitherto unknown class of strong gamma-ray emitters. Those MSP are characterised by very short periods and period derivatives (after being spun-up by a companion) and are located on the lower-left corner in Fig. 4.3. Beside these three groups, MS pulsars, YRL, and YRQ, the increase of sensitivity in longer data sets has revealed gamma-ray emission from new systems, such black widows and red back systems (see Bogdanov in this book). At TeV energies, the dominant gamma-ray

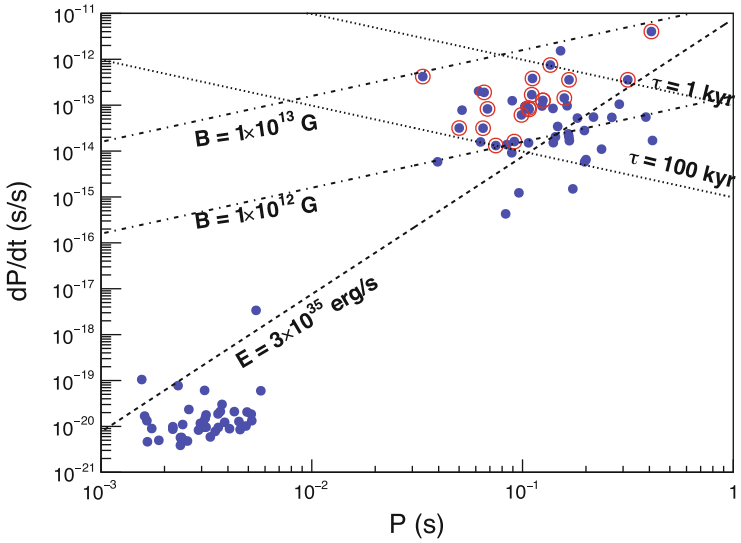

Fig. 4.3 P-$\dot{P}$ diagram corresponding to pulsars listed on the 2nd LAT pulsar catalog. LAT pulsars associated with TeV nebula are surrounded by a *red circle*. The estimate pulsar age τ, magnetic field strength B, and spin-down power E, obtained from the primary observable P and $\dot{P}$ are marked with *dashed-lines*

emission comes from the pulsar nebula. Indeed, PWNe are the most effective Galactic objects in producing very-high energy emission. In general, these very-high PWNe are related with young and energetic pulsars which power a magnetised nebula. In this scenario, particles are accelerated to very-high energies along their expansion into the pulsar surroundings and the interactions of relativistic leptons with the magnetic field and low energy radiation (of synchrotron origin, thermal, or microwave background), non-thermal radiation is produced from the lowest possible energies up to ∼100 TeV. On the other hand, for a few μG magnetic fields, young electrons create a small synchrotron nebula around the pulsar which should be visible in X-rays, in contrast of a often much larger TeV nebula, generated by inverse Compton processes. Typically only young pulsars ($\tau < 100$ kyrs) with large spin-down energy ($\dot{E} > 10^{33}$ erg s^{-1}) produce prominent PWNe. Concerning these TeV nebula, two kind of objects are usually considered according to their observational features: young systems such as the Crab nebula (Aleksić et al. 2015; Aharonian et al. 2006a; Archer and VERITAS Collaboration 2015), G0.9+0.1 (Aharonian et al. 2005a) or MSH 15–52 (Aharonian et al. 2005b), which often still lie within their composite supernova shell, and evolved (extended and resolved) systems, such as Vela X (Abramowski et al. 2012), HESS J1825−137 (Aharonian et al. 2006b) or HESS J1809−193 (Aharonian et al. 2007). The young systems show a good match with the morphology seen in X-rays, while in the latter group, very often the pulsar powering the TeV PWN is found offset with respect to the center of the TeV emission, with large size ratios between the X-ray and VHE gamma-ray emission

regions. The evolution of the SNR blast wave into an inhomogeneous ISM and/or the high velocity of the pulsar, together with a low magnetic field value ($\sim$5 μG), may explain these large offset as being the relic nebulae from the past history of the pulsar wind inside its host SNR.

The second *Fermi* pulsar catalog provides very valuable information when comparing the population of LAT pulsars and the TeV PWNe. The catalog registers the positions and characteristics of 117 pulsars (see Fig. 4.3), from which the distance, pulsar parameters, energetics and spectral energy distribution, can be extracted. To investigate possible links between these high-energy pulsars and their TeV nebulae, we used the population of PWNe presented by H.E.S.S., which includes PWNe lying on the inner part of the Galaxy but also objects on the outer regions reported by other experiments, which mainly lie on the galactic anti-center and the Cygnus region. From the 61 PWNe/Pulsars investigated, 34 are firmly identified as PWNe whereas for 27 sources, upper limits on the integral flux in the 1–10 TeV energy range of the order of $\sim 10^{-12}$ cm/s were derived. Out of the 34 TeV sources, 14 have been associated with bright, young, LAT pulsars. Table 4.1 shows the LAT pulsars for which a TeV nebula has been associated, together with their location in the Galaxy and their classification as radio loud or quiet.

In Fig. 4.3 we show the P-$\dot{P}$ diagram for the LAT pulsars in the catalog (in blue), where pulsars with an associated TeV nebula are marked with a red circle. These pulsars have rotational energies $\dot{E} > 3 \times 10^{35}$ erg/s as expected for typical pulsars associated to TeV nebulae. The dashed lines in Fig. 4.3 define the region of parameters derived from the period and period derivative corresponding to the pulsars associated to TeV nebulae. They are typically highly magnetised, with magnetic fields above 1×10^{12} G and relatively young, in a range of ages between $\sim$1

Table 4.1 LAT pulsars associated with TeV nebulae

LAT PSR	TeV PWN	l (°)	b (°)	Dist[a] (kpc)	Type
J0007+7303	J0007+7303	119.65	10.60	1.40	YRQ
J0205+6449	J0205+6449	130.72	3.08	1.96	YRL
J0534+2200	B0531+21	184.56	−5.78	2.0	YRL
J1016−5857	J1016−5857	284.08	−1.88	2.90	YRL
J1023−5746	J1023−5746	284.17	−0.41	8.00	YRQ
J1028−5819	J1028−5819	285.07	−0.46	2.33	YRL
J1119−6127	J1119−614	292.15	−0.54	8.40	YRL
J1357−6429	J1356−645	309.92	−2.51	2.50	YRL
J1420−6048	J1420−607	313.54	0.23	5.61	YRL
J1418−6058	J1418−609	313.31	0.11	1.60	YRL
J1718−3825	J1718−3825	348.95	−0.43	3.60	YRL
J1747−2958	J1747−2809	0.86	0.09	4.75	YRL
J1801−2451	B1800−21	8.40	0.15	5.22	YRL
J1907+0602	J1907+0602	40.08	−0.88	3.21	YRQ

[a]The distance corresponding to the LAT pulsars is assumed here

and 100 kyrs. No TeV PWN has been found around a millisecond pulsar, however, in the presence of a companion wind, TeV emission could be in principle expected (Bednarek et al. 2016).

4.4.1 Distribution of LAT Pulsars and TeV PWNe in the Galaxy

The distributions in the Galaxy of the LAT pulsars and TeV PWNe are shown in Fig. 4.4, in a two-dimensional projection. The figure also shows an schematic representation of the spiral arm of the Milky Way according to the parametrisation of Vallée (2008). The Galactic center position and the Sun position are marked with stars. On the left plot (Fig. 4.4a), the YRQ and YRL LAT pulsars are marked with grey crosses and the MSP ones with yellow crosses. The TeV PWNe positions are marked with blue circle and red inverted triangles, for the detected and non-detected ones, respectively. The ones with an associated LAT PSRs are marked with a light blue circle. For clarity, the right plot (Fig. 4.4b) shows only the LAT YRL and YRQ and the TeV sources with LAT counterpart. From the galactocentric distribution of LAT pulsars, it is clear that there is a observational bias towards a region between -10 and -5 kpc in the X-galactocentric coordinate and -5 kpc and 5 kpc in the Y-galactocentric coordinates. The TeV PWNe instead seem to be located in a wider region, clustering around the position of the Carina-Sagittarius arm. The Sagittarius arm is considered one of the minor spiral arm in our Galaxy, but hosts a large number of HII regions, young stars and giant molecular clouds. In fact, the TeV emission depends not only on the pulsar energetics but also on the surrounding medium, that provides the up-scattered photon field in the inverse Compton emission. It is reasonable then to believe that pulsars located in regions with large stellar activity are more likely to be bright in gamma-rays. This correlations was investigated by Pedaletti et al. (2015) and also pointed out by Torres et al. (2014). On the other hand, the LAT telescope suffers greatly from the large diffusion emission produced in the inner part of the Galaxy. That might explain the reduced number of LAT PSR close to the direction of the Galactic center, for X-galactocentric distance larger than -5 kpc. Note that the strong gamma-ray emission from pulsars allow the detection of very distant ones, whereas in the case of TeV PWN, a compromise between the size of the nebula (close nebulae might be too large to be detected with the current instruments FoV with enough sensitivity) and the intensity of the emission (not too far to be too faint) might also resulting on an observational biased towards distances between $\sim$2 and $\sim$5 kpc.

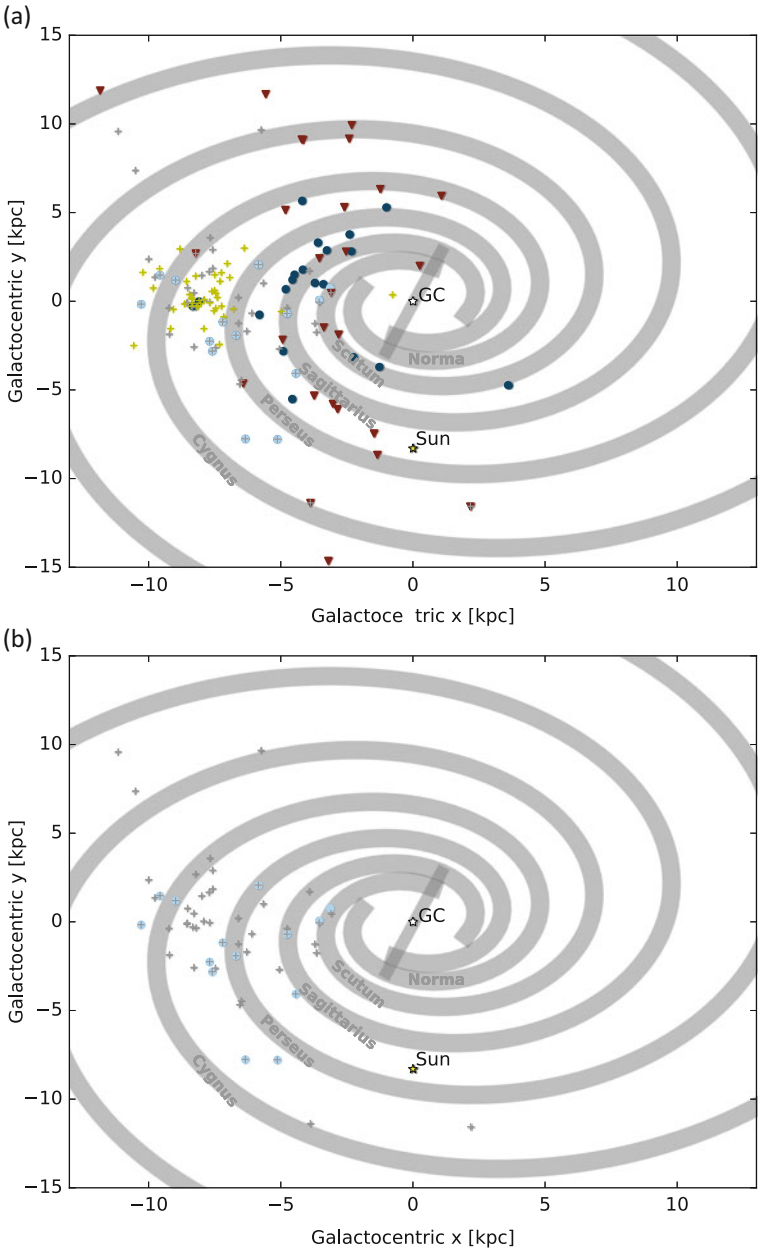

Fig. 4.4 At the *top* (**a**) two-dimensional projection of the positions of the LAT pulsars contained the 2nd *Fermi* Pulsar Catalog and the TeV PWNe (see text). The *grey crosses* mark the position of LAT YRQ and YRL pulsars whereas the *yellow* ones refer to MSP. The *blue dots* sign the TeV PWNe whereas we used *red inverted triangles* to mark the position of energetic pulsars for which an upper limit on steady TeV emission was provided. Finally the *light blue dots* mark TeV PWNe with an associated LAT pulsars. At the *bottom* (**b**) Only the *grey crosses* (LAT YRQ and YRL) and *blue circles* (TeV PWN with associated LAT PSR) are indicated for clarity

4.4.2 Energetics

The study of the spectral energy distribution should in principle serves as a bridge between pulsars and PWNe. The pulsar energy reservoir ($\dot{E}$) is shared between the pulsed emission and the radiation emitted by the nebula. However, the different dimensions and time scales of the two objects together with the lack of accurate information about magnetic field distribution and strength in the small and large scale, and photon fields present in the surrounding medium, render a complex picture with non-trivial solution. The spectral energy distribution of pulsed gamma-ray emission from most pulsars peak around a few GeV, above which the flux quickly decreases exponentially with energy. This exponential cutoff is expected when synchrotron-curvature is appealed to work in the pulsar magnetosphere, where particles reach a maximum energy limited by either magnetic absorption or radiation losses. Nevertheless, longer observations of bright GeV pulsars show an unexpected deviation from a pure exponential cutoff, questioning the previous established mechanisms (Li et al. 2016; Ahnen et al. 2016; Ansoldi et al. 2016; Breed et al. 2016). This deviation observed in phase-resolved spectra can arise from the caustic emission (Dyks and Rudak 2003; Viganò et al. 2015; Prosekin et al. 2013), i.e, overlapping of photons emitted at different heights and along different magnetic field lines or from a different interplay between acceleration and energy lose mechanisms. In particular, two pulsars have been recently detected by Cherenkov telescopes: deep observations of the Crab pulsar have revealed a second component of pulsed radiation that extends from GeV energies to above a few TeV (Ansoldi et al. 2016; VERITAS Collaboration et al. 2011). This unexpected result has drawn a large attention in the astrophysics community and it has triggered a large number of research theoretical projects aiming to unveil the mechanisms powering GeV/TeV pulsars and their winds; a second pulsar was detected using the H.E.S.S. II telescope above 20 GeV and up to 120 GeV, also departing from an exponential cutoff shape (Breed et al. 2016).

The gamma-ray luminosity in pulsars L_γ can be calculated from the observed flux G_{100} above 100 MeV, when the distance d is known, assuming a given beaming factor f_Ω, i.e. the fraction of the radiation that reaches the observer. The luminosity thus can be expressed as $L_\gamma = 4\pi d^2 f_\Omega G_{100}$, which introduces an unknown factor corresponding to the fan-like beam size when calculating the efficiency of the radiation transferred from the pulsar $\dot{E}$ to the pulsed emission does. A general trend close to $L_\gamma \propto \dot{E}$ has been observed, although Pierbattista et al. (2016) show that the range of variation depends on the pulsar type and magnetospheric model assumed. In the case of PWNe, the emitting electrons responsible for the TeV emission do not suffer from very severe radiative losses as in the case of i.e. X-ray nebulae, and the majority of them may survive from (and hence probe) early epochs of the PWNe evolution. Therefore the TeV emission observed corresponds

to the accumulation of high-energy electrons from different evolution times. This interpretation has been further supported by the discovery of the spectral softening of the very-high energy nebulae HESS J1825−137 and HESS J1303−631 as a function of the distance from the pulsar (Aharonian et al. 2006b; Abramowski et al. 2012). The spectrum of PWNe is mostly determined by the accumulation of the injection electron spectrum but also by the nature of the target photon field for the inverse Compton scattering. Torres et al. (2014) studied the spectral energy distribution of 10 PWNe, modelling their emission using a time-dependent description of the nebulae's electron population. The injection parameters derived from the TeV modelling do not appear to be particularly correlated with the pulsar properties. On the other hand, Abeysekara and Linnemann (2015) studied the correlation between the LAT pulsars and their corresponding TeV PWNe in terms of luminosity. Abeysekara and Linnemann (2015) found a linear correlation (R=0.82) between the PSR luminosity (assuming a beaming factor of f_Ω) and TeV PWNe luminosity, which contrary to the pulsar one, comprised a 4π area.

We investigated the relation ship between the TeV PWN luminosity and the various parameters than defined the pulsed emission at GeV, namely, the spin-down energy of the pulsar $\dot{E}$, the GeV luminosity L_γ, the spectral index and the pulsar efficiency, defined as the fraction of rotational energy transferred to the GeV pulsed emission. The TeV PWNe luminosity has been compared with the pulsar rotational energy, resulting on a lack of dependency between the two parameters (Mattana et al. 2009). However, the larger sample studied by Klepser et al. (2016) resulted on a clear correlation of luminosity with pulsar spin-down, suggesting a dependency of $L_{1-10\mathrm{TeV}} = \dot{E}^{0.6\pm0.2}$. This correlation is somehow dimmed when focusing only in the LAT pulsars sample. The dashed-black line on Fig. 4.5 top shows such relation. The black-dashed line results from a linear fitting which clearly does not represent well the population. However, it is interesting to note that the fit is mainly affected by two young pulsars, the Crab and 3C58. The dashed-dotted line indicates a certain trend resulting from fitting the population excluding the two later, although the large errors prevent a claim in this direction. Likewise, a trend seems to be present when comparing the PWNe luminosity with the pulsar one, somehow expected from the correlation between the pulsar luminosity and the spin-down power. Note again, that we do not claim at this stage any quantitative correlation at this stage. When comparing the luminosity with the pulsar efficiency, no tendency or correlation is observed, likewise the spectral index. This is expected since the two parameters rather depend on the propagation and geometry of particles within the magnetosphere and not on the injection spectrum or total pulsar energetics.

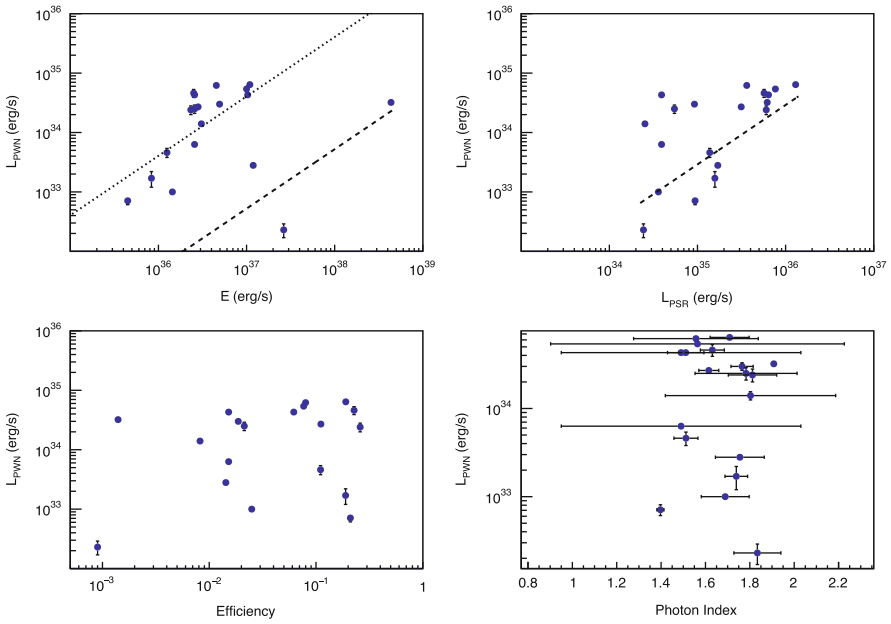

Fig. 4.5 Correlation between the TeV PWN Luminosity (see Table 4.1 and different parameters that define pulsars spectral energy distribution. The *top panels* show the correlation with the spin-down energy $\dot{E}$ and the pulsar luminosity (*left* and *right* respectively). The *bottom panels* show the TeV luminosity as compare with the pulsar efficiency and the pulsed spectral photon index (*left* and *right*)

4.5 New Type of Pulsars and Pulsar Wind Nebula

Beside MSP pulsars, the LAT has revealed new type of compact accelerators to high energies previously unknown. Among them are the transitional millisecond pulsars (such i.e. PSR J1023+0038 (Tam et al. 2010), see Fig. 4.6, or XSS J12270−4859 (Johnson et al. 2010)), black window systems (such 2FGL J1311.7−3429 (Romani 2012)) or, less certain, accreting millisecond pulsar such SAX J1808.4−3658 (de Oña Wilhelmi et al. 2016). The discovery of millisecond pulsars switching between states powered either by the rotation of their magnetic field or by the accretion of matter has recently proved the tight link shared by millisecond radio pulsars and isolated neutron stars in low-mass X-ray binaries. Those transitional millisecond pulsars also show an intermediate state in which the neutron star is likely surrounded by an accretion disk and emits coherent X-ray pulsations. In that intermediate state, the X-ray emission does not reach the level observed on accreting neutron stars, but at GeV energies it emits a large luminosity compared to the previous state. Several possibilities have been suggested to explain the complex phenomenology observed on those systems, implying acceleration of electrons in the pulsar wind or/and the intra-shock regime produced by the disk (Stappers et al. 2014; Takata et al. 2014;

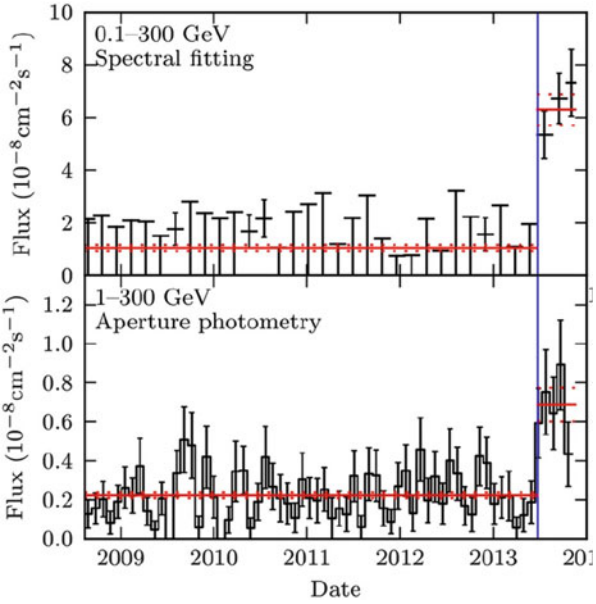

Fig. 4.6 Gamma-ray photon flux from PSR J1023+0038 (Stappers et al. 2014). *Top panel*: the 100 MeV to 300 GeV flux determined by spectral fitting. *Bottom panel*: the 1–300 GeV flux determined by aperture photometry, with Poisson uncertainties

Coti et al. 2014). In general, the new objects type detected by LAT show a spectral energy distribution characterised by a power law function plus and exponential cutoff at a few GeV. Radiation at TeV energies, if existing, should thus be produced by a new inverse Compton component. Observations at very-high energy (Aliu et al. 2016) of PSR J1023+0038 have resulted on upper limits, imposing limits on the maximum magnetic field strength in the synchrotron/inverse Compton region. The most promising results at very-high energy concerning this new type of sources are HESS J1808−204 (see Fig. 4.7) (Abdalla et al. 2016), TeV J2032+4130 (Albert et al. 2008) (in Fig. 4.8) and HESS J1747−248 (H.E.S.S. Collaboration et al. 2011) (in Fig. 4.9). The first is an extended very-high gamma-ray emission towards SGR1806−20 and the stellar cluster Cl* 1806−20, the second is an extended source that has been associated with an evolved pulsar which is gravitationally linked to a massive star companion, and the third TeV source is positionally in agreement with the globular cluster Terzan 5. The magnetar SGR 1806−20 is one of the most prominent and burst-active soft gamma repeaters. The emission detected at TeV energies is coincident with the synchrotron radio nebula G10.0−0.3 which is believed to be powered by LBV 1806−20. It is also in agreement with the position of the GeV source 3FGL J1809.2−2016c (Yeung et al. 2016). The GeV and TeV maps show a very good morphological agreement between the two sources, whereas the spectrum extends as a power-law function from a few hundreds of MeV to a few tens of TeV. The WR star LBV 1806−20 that belongs to the cluster Cl* 1806−20, which

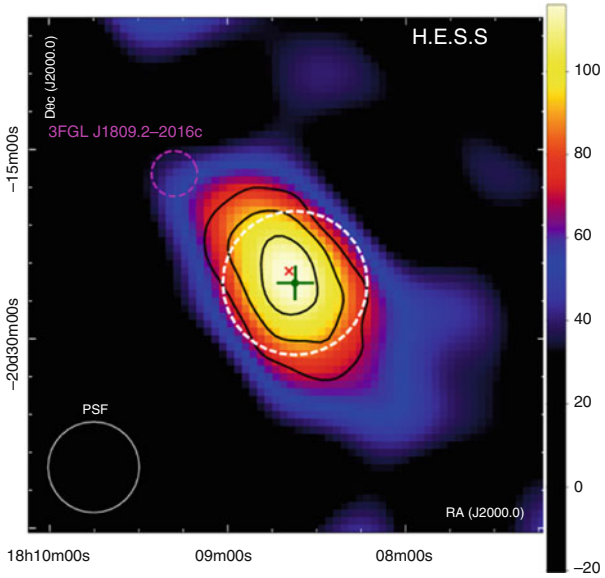

Fig. 4.7 H.E.S.S. exposure-corrected excess counts image of HESS J1808−204 towards the stellar cluster Cl* 1806−20 (*red cross*), containing SGR 1806−20 and LBV 1806−20 (Abdalla et al. 2016)

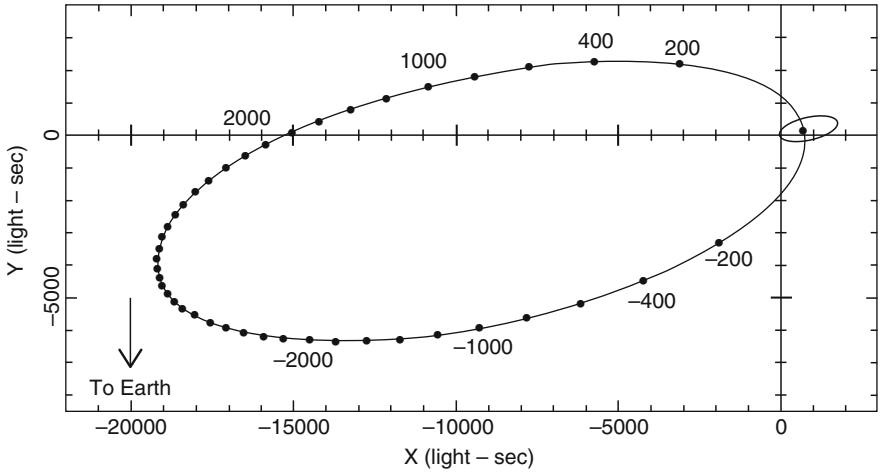

Fig. 4.8 Schematic diagram showing the approximate orbital motions of PSR J2032+4127 and its Be-star companion MT91 213 (Lyne et al. 2015)

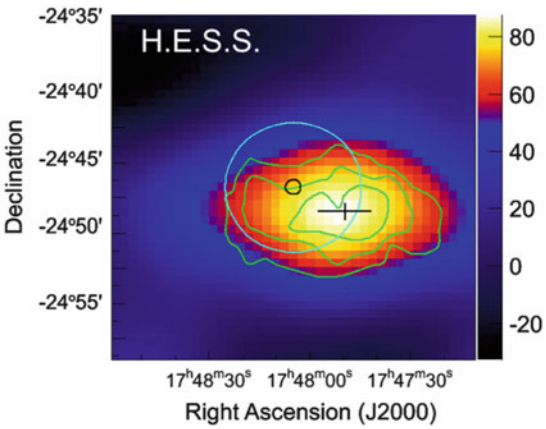

Fig. 4.9 Gamma-ray image of the Terzan 5 region (H.E.S.S. Collaboration et al. 2011). *Green lines* give 4–6 sigma significance contours. The *circles* show the half-mass radius of about 30 arcseconds (in *black*) and the larger tidal radius of 4.6 arcminutes (in *cyan*) of the GC

displays a kinetic stellar wind luminosity of $L_W=10^{38}$ erg/s could easily account for the TeV luminosity via hadronic or leptonic mechanisms. At GeV energies, Yeung et al. (2016) have claimed variability from the direction of the magnetar. The association of the GeV and TeV emission with the magnetar, if confirmed, will entail the first TeV pulsar wind nebula powered by a magnetic-driven wind. H.E.S.S. has also detected very-high energy emission from the direction of the cluster Terzan 5 (H.E.S.S. Collaboration et al. 2011), which is especially rich in eclipsing binary systems among globular clusters. The origin of the emission was proposed to be related to the combined effect of the millisecond pulsars winds or to one particular one. Unfortunately, the TeV emission is displaced with respect the GeV one, and a clear association is still on hold. Searches for VHE emission from the globular clusters 47 Tucanae (Aharonian et al. 2009), M5, M15 (McCutcheon 2009), and M13 (Anderhub et al. 2009; McCutcheon 2009) have only resulted on upper limits. Finally, the unidentified source TeV J2032+4130 has been recently associated with the LAT pulsar PSR J2032+4127. PSR J2032+4127 is an energetic pulsar with a X-ray nebula associated (Murakami et al. 2011), and the TeV-GeV association could be easily established except, perhaps, for the pulsar age (0.11 Myr). However, radio observations have shown that the pulsar is in a highly-eccentric binary ($\sim$100 yrs) system with a 15-solar-mass Be star, MT91 213 (Lyne et al. 2015). That renders the association between the LAT pulsar and the TeV source an intriguing aspect, since it will imply either an extremely fast ($<$100 years) evolution of a high-energy nebula or a nebula created being disrupted only by the companion every pass on the periastron. The next passage which will be happening next year will shed some light on this interesting object.

4.6 Prospects and Conclusions

The association with energetic LAT pulsar powering TeV PWNe is supported by a combination of positional and morphological evidence, multi-wavelength observations, and energy arguments. The two populations constitute the most numerous class of identified Galactic high and very-high energy gamma-ray sources respectively. However, only half of the TeV PWNe candidates have an associated LAT pulsar. This is partially due to an observational bias (see Fig. 4.3) towards regions of the Galaxy which are not too contaminated by the diffuse Galactic background, or simply to the fact that the large size of the TeV sources often hinders a clear association with a unique GeV pulsar. However, it seems like luminosity of the TeV PWNe which have a LAT pulsar associated weakly depends on the pulsed GeV luminosity. The large dispersion (see Fig. 4.4) can be explained the dependency of the pulsed emission on the beaming factor and/or by the dependency of the PWN luminosity on many parameters, such photon field, age, etc.

At TeV energies, deep exposures unveiling cooling processes and complex morphology with sensitive instrument such the future CTA, will allow a clear determination of the key parameters that rule the high and very-high energy emission. Likewise, future observations will also allow a complete population study of the Galaxy (up to $\sim$15 pc, see de Oña-Wilhelmi et al. 2013) and an unbiased study of the correlation between LAT pulsar population and TeV PWN sources. These information will be crucial to develop time-dependent morphological models, which will finally reveal the intrinsic connections between the compact $\sim 10^6$ cm radius pulsars and the enormous tens-of-parsec extension nebulae.

References

Abdalla, H., Abramowski, A., Aharonian, F., et al.: arXiv:1606.05404 (2016)
Abdo, A.A., Ackermann, M., Ajello, M., et al.: Science **325**, 840 (2009)
Abdo, A.A., Ajello, M., Allafort, A., et al.: Astrophys. J. Suppl. Ser. **208**, 17 (2013)
Abeysekara, A.U., Linnemann, J.T.: Astrophys. J. **804**, 25 (2015)
Abramowski, A., Acero, F., Aharonian, F., et al.: Astron. Astrophys. **548**, A38 (2012)
Aharonian, F., Akhperjanian, A.G., Aye, K.-M., et al.: Astron. Astrophys. **432**, L25 (2005a)
Aharonian, F., Akhperjanian, A.G., Aye, K.-M., et al.: Astron. Astrophys. **435**, L17 (2005b)
Aharonian, F., Akhperjanian, A.G., Bazer-Bachi, A.R., et al.: Astron. Astrophys. **457**, 899 (2006a)
Aharonian, F., Akhperjanian, A.G., Bazer-Bachi, A.R., et al.: Astron. Astrophys. **460**, 365 (2006b)
Aharonian, F., Akhperjanian, A.G., Bazer-Bachi, A.R., et al.: Astron. Astrophys. **472**, 489 (2007)
Aharonian, F., Akhperjanian, A.G., Anton, G., et al.: Astron. Astrophys. **499**, 273 (2009)
Aharonian, F.A., Bogovalov, S.V., Khangulyan, D.: Nature **482**, 507 (2012)
Ahnen, M.L., et al.: Astron. Astrophys. **591**, A138 (2016)
Albert, J., Aliu, E., Anderhub, H., et al.: Astrophys. J. **675**, L25 (2008)
Aleksić, J., Ansoldi, S., Antonelli, L.A., et al.: J. High Energy Astrophys. **5**, 30 (2015)
Aliu, E., Archambault, S., Archer, A., et al.: arXiv:1609.01692 (2016)
Anderhub, H., Antonelli, L.A., Antoranz, P., et al.: Astrophys. J. **702**, 266 (2009)
Ansoldi, S., et al.: Astron. Astrophys. **585**, A133 (2016)

Archer, A., VERITAS Collaboration: APS April Meeting Abstracts (2015)
Atwood, W.B., et al.: Astrophys. J. **697** 1071 (2009)
Bednarek, W., Sitarek, J., Sobczak, T.: Mon. Not. R. Astron. Soc. **458**, 1083 (2016)
Breed, M., Venter, C., Harding, A.K.: arXiv, arXiv:1607.06480 (2016)
Bogovalov, S., Tsinganos, K.: Mon. Not. R. Astron. Soc. **357**, 918 (2005)
Caraveo, P.A.: Annu. Rev. Astron. Astrophys. **52**, 211 (2014)
Cerutti, B., Philippov, A.A., Spitkovsky, A.: Mon. Not. R. Astron. Soc. **457**, 2401 (2016)
Contopoulos, I.: Mon. Not. R. Astron. Soc. **463**, L94 (2016)
Coti Zelati, F., Baglio, M.C., Campana, S., et al.: Mon. Not. R. Astron. Soc. **444**, 1783 (2014)
de Oña Wilhelmi, E.: Am. Inst. Phys. Conf. **1357**, 213 (2011)
de Oña-Wilhelmi, E., Rudak, B., Barrio, J.A., et al.: Astropart. Phys. **43**, 287 (2013)
de Oña Wilhelmi, E., Papitto, A., Li, J., et al.: Mon. Not. R. Astron. Soc. **456**, 2647 (2016)
Del Zanna, L., Amato, E., Bucciantini, N.: Astron. Astrophys. **421**, 1063 (2004)
Del Zanna, L., Volpi, D., Amato, E., Bucciantini, N.: Astron. Astrophys. **453**, 621 (2006)
Dyks, J., Rudak, B.: Astrophys. J. **598**, 1201 (2003)
Fang, J., Zhang, L.: Astron. Astrophys. **515**, A20 (2010)
Gallant, Y.A., et al.: Am. Inst. Phys. Conf. **983**, 195 (2008)
Gelfand, J.D., Slane, P.O., Zhang, W.: Astrophys. J. **703**, 2051 (2009)
Gonthier, P.L., Story, S.A., Clow, B.D., Harding, A.K.: Astrophys. Space Sci. **309**, 245 (2007)
Grégoire, T., Knödlseder, J.: Astron. Astrophys. **554**, A62 (2013)
Grenier, I.A., Harding, A.K.: C. R. Phys. **16**, 641 (2015)
H.E.S.S. Collaboration, Abramowski, A., Acero, F., et al.: Astron. Astrophys. **531**, L18 (2011)
H.E.S.S. Collaboration, Abramowski, A., Acero, F., et al.: Astron. Astrophys. **548**, A46 (2012)
Johnson, T.J., Ray, P.S., Roy, J., et al.: Astrophys. J. **806**, 91 (2015)
Johnson, T.J., Smith, D.A., Kerr, M., den Hartog, P.R., Fermi Large Area Telescope Collaboration, Timing Consortium P., Search Consortium P.: Am. Astron. Soc. **223**, 153.02 (2014)
Kalapotharakos, C., Kust Harding, A., Kazanas, D., Brambilla, G.: Am. Astron. Soc. **227**, 423.01 (2016)
Kargaltsev, O., Rangelov, B., Pavlov, G.G.: arXiv, arXiv:1305.2552 (2013)
Kennel, C.F., Coroniti, F.V.: Astrophys. J. **283**, 710 (1984)
Klepser, S., Gallant, Y., Mayer, M., Valerius, K., For The H.E.S.S. Collaboration: Proc. 35th ICRC, Busan, South Korea, PoS(ICRC2017)731. arXiv:1707.04024 (2017)
Komissarov, S.S., Lyubarsky, Y.E.: Mon. Not. R. Astron. Soc. **344**, L93 (2003)
Komissarov, S., Lyubarsky, Y.: Astrophys. Space Sci. **293**, 107 (2004)
Li, J., Torres, D.F., de Ona Wilhelmi, E., Rea, N., Martin, J.: Astrophys. J. **831**, 19 (2016)
Lyne, A.G., Stappers, B.W., Keith, M.J., et al.: Mon. Not. R. Astron. Soc. **451**, 581 (2015)
Lyubarsky, Y.E.: Mon. Not. R. Astron. Soc. **329**, L34 (2002)
Martín, J., Torres, D.F., Rea, N.: Mon. Not. R. Astron. Soc. **427**, 415 (2012)
Mattana, F., Falanga, M., Götz, D., et al.: Astrophys. J. **694**, 12 (2009)
McCutcheon, M., for the VERITAS Collaboration: arXiv:0907.4974 (2009)
Mochol, I., Pétri, J.: Mon. Not. R. Astron. Soc. **449**, L51 (2015)
Murakami, H., Kitamoto, S., Kawachi, A., Nakamori, T.: Publ. Astron. Soc. Jpn. **63**, S873 (2011)
Muslimov, A.G., Harding, A.K.: Astrophys. J. **617**, 471 (2004)
Nolan, P.L., et al.: Astron. Astrophys. Suppl. Ser. **120**, 61 (1996)
Pétri, J.: Astron. Astrophys. **574**, A51 (2015)
Pedaletti, G., de Oña Wilhelmi, E., Torres, D.F., Natale, G.: J. High Energy Astrophys. **5**, 15 (2015)
Pierbattista, M., Harding, A.K., Gonthier, P.L., Grenier, I.A.: Astron. Astrophys. **588**, A137 (2016)
Porth, O., Komissarov, S.S., Keppens, R.: Mon. Not. R. Astron. Soc. **438**, 278 (2014)
Prosekin, A.Y., Kelner, S.R., Aharonian, F.A.: arXiv:1305.0783 (2013)
Ray, P.S., Parkinson, P.M.S.: Astrophys. Space Sci. Proc. **21**, 37 (2011)
Romani, R.W.: Astrophys. J. **754**, L25 (2012)
Romani, R.W., Yadigaroglu, I.-A.: Astrophys. J. **438**, 314 (1995)
Spitkovsky, A.: Astrophys. J. **648**, L51 (2006)
Stappers, B.W., Archibald, A.M., Hessels, J.W.T., et al.: Astrophys. J. **790**, 39 (2014)

Takata, J., Shibata, S., Hirotani, K., Chang, H.-K.: Mon. Not. R. Astron. Soc. **366**, 1310 (2006)
Takata, J., Li, K.L., Leung, G.C.K., et al.: Astrophys. J. **785**, 131 (2014)
Tam, P.H.T., Hui, C.Y., Huang, R.H.H., et al.: Astrophys. J. **724**, L207 (2010)
Tanaka, S.J., Takahara, F.: Mon. Not. R. Astron. Soc. **429**, 2945 (2013)
Tavani, M., AGILE Team: Nucl. Instrum. Methods Phys. Res. A **630**, 7 (2011)
Tchekhovskoy, A., Philippov, A., Spitkovsky, A.: Mon. Not. R. Astron. Soc. **457**, 3384 (2016)
Thompson, D.J., Bertsch, D.L., O'Neal Jr., R.H.: Astrophys. J. Suppl. Ser. **157**, 324 (2005)
Torres, D.F., Cillis, A., Martín, J., de Oña Wilhelmi, E.: J. High Energy Astrophys. **1**, 31 (2014)
Vallée, J.P.: Astrophys. J. **681**, 303–310 (2008)
VERITAS Collaboration, Aliu, E., Arlen, T., et al.: Science **334**, 69 (2011)
Viganò, D., Torres, D.F., Martín, J.: Mon. Not. R. Astron. Soc. **453**, 2599 (2015)
Watters, K.P., Romani, R.W.: Astrophys. J. **727**, 123 (2011)
Weekes, T.C., et al.: Astrophys. J. **342**, 379 (1989)
Yeung, P.K.H., Kong, A.K.H., Tam, P.H.T., et al.: Astrophys. J. **827**, 41 (2016)